

Development of 3-DOF lifting platform for hilly orchards

Duan Zhenhua^{1,2}, Qiu Wei^{1,2}, Ding Weimin^{1,2*}, Liu Yande²,
Ouyang Yuping², Huang Liang¹

(1. College of Engineering, Nanjing Agricultural University, Nanjing 210031, China;

2. Co-Innovation Center of the Intelligent Management and Equipment for Orchard on the Hilly Land in South China, Nanchang, 330013, China)

Abstract: In order to improve the mechanization degree of operations such as picking, pruning, and bagging in hilly orchards, and solve the problems of insufficient operating capabilities and low operating range of current orchard lifting machinery in complex terrains, a 3-DOF lifting platform for hilly orchards was developed. The main structure and operating parameters such as operating height, operating radius, and operating range were determined by the geometric parameters of fruit trees and theoretical analysis. To evaluate the performance of the platform, experiments of the prototype including operating parameters experiment, operating effect on fruit trees experiment, leveling experiment and tilting stability experiment were carried out. The experimental results indicated that lifting, rotating and leveling actions were smooth at low speed, the maximum operating height was 1.2 m, and at a maximum operating radius of 1.42 m, the lifting device could rotate 360° with an operating range of 3.6 m². In addition, the leveling error was less than 0.4°, which is negligible and the leveling device can be considered to have a relatively high accuracy. The maximum tilting angle when the platform was at any parked position, equipped with different loads and at various operating heights, was 19.3° to 30°, which were consistent with the design requirements. The maximum tilting angle could also adapt to slope conditions of 5° to 20° in hilly orchards. The proposed 3-DOF lifting platform for hilly orchards has a better tilting stability performance compared to contemporary machinery. This study can provide reference for future design of lifting machinery in hilly orchards based on the characteristics of terrain and fruit tree planting.

Keywords: 3-DOF lifting platform, orchard mechanization, hilly land, lifting platform, operating parameters, leveling, experiments

Citation: Duan, Z. H., W. Qiu, W. M. Ding, Y. D. Liu, Y. P. Ouyang, and L. Huang. 2017. Development of 3-DOF lifting platform for hilly orchards. *International Agricultural Engineering Journal*, 26(3): 37–48.

1 Introduction

Mechanization of orchard activities is not only important for the development of the fruit industry, but is also an important part of agricultural production mechanization (Chang et al., 2013; Hong et al., 2010). In recent years, with the rapid development of the orchard industry, more large-scale and standardized orchards are built in China. These orchards have certain requirements on the shape of fruit trees, and have a larger row spacing and plant spacing. This promotes the use of adaptable

multi-functional orchard management machinery, and provides a push for orchard mechanized operations at the same time (Wang et al., 2013; Li et al., 2012). This mechanization also increases the efficiency in traditional orchard production processes such as picking, pruning, bagging, etc. which were mostly carried out using ladders, stepping on stools and other modes of artificial climbing operation, which were not only labor intensive, but also had greater security risks.

Because of proper planning, flatness, and maneuverability of machinery in orchards in European and American countries were better, which resulted in the earlier adoption of orchard lifting platforms in these countries. This also led lifting platforms to mainly use the wheel travel mechanism, which were suitable for operating in plain terrain (Liu et al., 2015). British Genie

Received date: 2017-03-29 Accepted date: 2017-07-03

* Corresponding author: Ding Weimin, Ph.D., Professor of Department College of Engineering, Nanjing Agricultural University, Nanjing 210031, China. Email: wmding@njau.edu.cn, Tel: 025-5860 6502.

developed Gr12, Gr15 and Gr20 models of electric wheel type lifting platform and Seymour developed Windegger picking devices wheel lifting platform (Tang et al., 2006); American Nelson developed tree squirrel pruning and picking tower for orchards; Australia Crendon developed lifting platform for picking the mango and avocado; Japan Shikoku Agricultural Experiment Station developed crawler chassis self walking type picking vehicle (Wang et al., 2014). In recent years, many research institutions and companies have also developed a few lifting platforms for orchards in China. Xinjiang Institute of Mechanization developed a multi-functional orchard machine (Liu et al., 2009); Beijing Agricultural Machinery Test and Accreditation Station developed a small multi-function remote control power platform (Wang, 2011); Hebei Agricultural University developed a crawler multifunctional orchard operating platform (Sun, 2012; Wang, 2013); Shandong Agricultural University developed a hanging operating platform for hilly orchards (Wang, 2013); Hunan Agricultural University developed a lifting platform in citrus orchards (Liu, 2013), etc. Although these current machineries make the lifting operation possible, most of them do not have the ability to work in hilly orchards, and cannot adapt to the rugged terrain conditions. The scissor structure that was mainly used in these machineries could only lift in the vertical direction. In addition, limited by the size of the worktable, the operating range in the horizontal plane was generally small, usually between 0.64 m² and 1.5 m². As a result, these lifting platforms had to move frequently to change the operating position for some fruit trees with larger crown. This not only made the operation tedious, but also increased the risk on hilly lands.

Considering the structure, working principle, and problems associated with the current lifting platforms used in orchards, this study developed a 3-DOF lifting platform for hilly orchards to realize operations under complex terrain conditions and improve the overall production efficiency.

2 Design requirements and structural principle

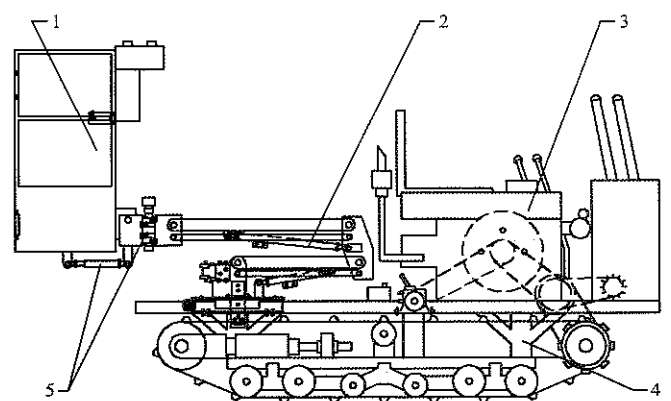
2.1 Design requirements

Barring a few exceptions, a large scale and centralized

planting pattern when adopted in hilly orchards, has certain requirements on row spacing, plant spacing and fruit tree shape. Thus, the orchard lifting platform should be adapted to the planting environment of the hilly land and the orchard management practices, and in line with the operating requirements of picking, pruning, bagging, etc. which are stated as follows. The operating height and operating radius should be adapted to the height and crown of different fruit trees, and at the same time have a larger operating range. The manned worktable should have sufficient carrying capacity to transfer fruits, branches, leaves, etc. conveniently. In addition, the lifting platform should be usable on sloping fields with slope angle ranging from 5° to 20° with the manned worktable being horizontally leveled.

2.2 Main structure

The proposed 3-DOF lifting platform mainly consists of manned worktable, lifting device, power device, walking device and leveling device, as is shown in Figure 1. The lifting device is mainly composed of a folding-arm, slewing bearing, lifting hydraulic cylinder, hydraulic pump station and an electromagnetic valve group. The leveling device consists of leveling cylinder and leveling turbo-worm. The walking device adopts an agricultural crawler chassis, which has the advantages of compact structure, large ground connect area, small turning radius, and the ability to cross a ditch ridge (Zhang et al., 2014; Zhao et al., 2014; Cao et al., 2007). The parameters of the lifting platform are summarized in Table 1.



1. Manned worktable 2. Lifting device 3. Power device 4. Walking device
5. Leveling device

Figure 1 Diagram of 3-DOF lifting platform for hilly orchards

Table 1 Parameters of 3-DOF lifting platform for hilly orchards

Parameters	Value
Dimensions (L×W×H), mm	2730×1500×1900
Dimensions of manned worktable (L×W×H), mm	500×1000×1000
Weight, kg	1531.5
Maximum load, kg	150
Power, kW	16.2
Angle of rotating, °	360
Angle of leveling, °	±25

2.3 Working principle

When the lifting platform is moving in an orchard, the driver can control the joystick to realize forward, backward, and turning movements using different gears. The operator standing on the manned worktable can also reach a proper operating position by controlling the lifting device to lift and rotate. Additionally, the manned worktable can be leveled by the leveling device based on a bubble level (LJD13060C) when the ground is uneven.

The leveling principle: taking into account, the effect of different operating heights and different operating radii on the manned worktable level, the leveling cylinder and the leveling turbo-worm are put into operation to level the worktable through movements in all four directions.

As is shown in Figure 2, coordinate systems $oxyz$, $o_1x_1y_1z_1$, and $o_2x_2y_2z_2$ are set up on the basis of the horizontal ground, the lifting platform and the manned worktable, respectively. When the lifting platform is parked at any location with an angle α'' to the slope, which in turn has an angle α and α' with the x axis and y axis, respectively, the lifting device makes a rotational angle ω , with the lower-arm and upper-arm having angles

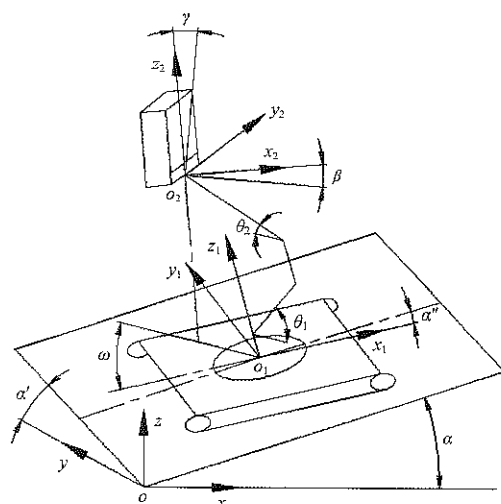


Figure 2 Schematic diagram of the leveling principle

θ_1 and θ_2 in the horizontal direction post lifting. The operating position of the manned worktable is can be determined by the angles $\alpha, \alpha', \alpha'', \omega, \theta_1$ and θ_2 . Under the coordinate system $o_2x_2y_2z_2$, the manned worktable has dip angle β and γ in the horizontal and vertical direction, respectively. The operator can control the leveling device to level at different operating positions using a bubble level installed on the control box.

3 Design of key parts

3.1 Lifting device design

3.1.1 Determination of operating height and radius

Figure 3 shows the relationship between the operation parameters of the lifting platform and the geometric parameters of fruit trees, from where the operating height and radius were determined using row spacing ($2s$), tree height (H), and tree crown (d). Where in this figure, h is the operating height, m; R is the operation radius, m; H is the tree height, m; H_1 is the trunk height, m; d is the diameter of tree crown, m; s is half of row spacing, m; h_1 is the height from the ground without lifting, m; h_2 is the average operating height of operator, m; θ_1 is lifting angle of lower-arm, (°); θ_2 is lifting angle of upper-arm, (°); l_1 is the length of lower-arm, mm; l_2 is the length of upper-arm, mm; l_3 is the length of mounting distance on the middle-arm between lower-arm and upper-arm in the horizontal direction, mm; l_4 is the length of leveling device, mm; and l_5 is the length of manned worktable, 500 mm.

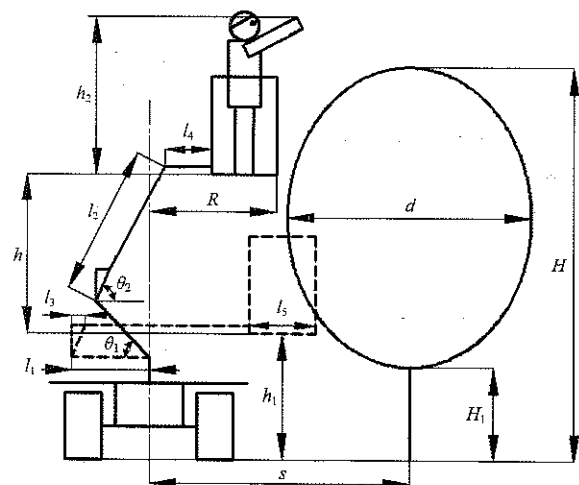


Figure 3 Schematic diagram of the lifting operation

The operating height and radius need to satisfy Equations (1) and (2), respectively:

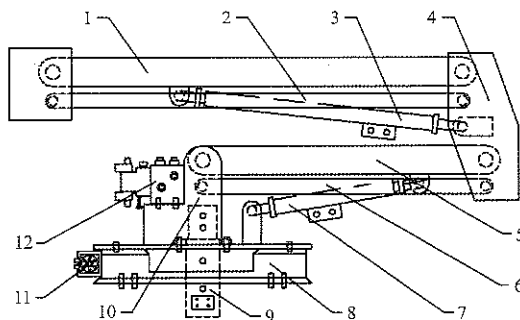
$$h = H - h_1 - h_2 \quad (1)$$

$$R = s - 0.5d \quad (2)$$

Accurate data of geometric parameters of fruit trees were collected by visiting orchards in hilly areas in Jiangxi Province and summarizing the results of previous studies (Qiu et al., 2012; Liu et al., 2014; Ding et al., 2013; Zhou et al., 2015; Qiu et al., 2016). It could be summarized that row spacing varied from 4 m to 6 m, plant spacing varied from 2 m to 4 m, tree height varied from 3 m to 3.8 m, tree crown varied from 1.5 m to 3 m, trunk varied from 0.4 m to 1 m, and the angle of slope varied from 5° to 20°. It had been known that h_1 was 0.9 m and h_2 was 1.7 m. Substituting these values in Equations (1) and (2) and solving them shows that the operating height and radius should be from 0.4 m to 1.2 m and from 1.3 m to 1.5 m, respectively. Therefore, the effective operating height and radius of lifting platform were chosen as 1.2 m (maximum value) and 1.4 m (average value).

3.1.2 Lifting mechanism

The lifting mechanism was developed as a folding-arm system with the advantages being a larger range and more operational flexibility compared to other lifting forms such as the scissors mechanism (Miao et al., 2013). As is shown in Figure 4, both ends of the upper-arm cylinder and lower-arm cylinder were connected with the middle-arm and upper-arm, base and lower-arm, respectively. The upper-arm linkage and lower-arm linkage ensured that the manned worktable was always parallel with the base, which was fixed on the slewing bearing. In addition, the base was also connected to the solenoid valve group and the central swivel joint.



1. Upper-arm 2. Upper-arm linkage 3. Upper-arm cylinder 4. Middle-arm 5. Lower-arm 6. Lower-arm linkage 7. Lower-arm cylinder 8. Slewing bearing 9. Central swivel joint 10. Base 11. Rotating hydraulic motor 12. Solenoid valve group

Figure 4 Structural schematic of the lifting device

As per the geometric relationship in the lifting mechanism (Figure 3), the operating height and radius satisfy the following equations:

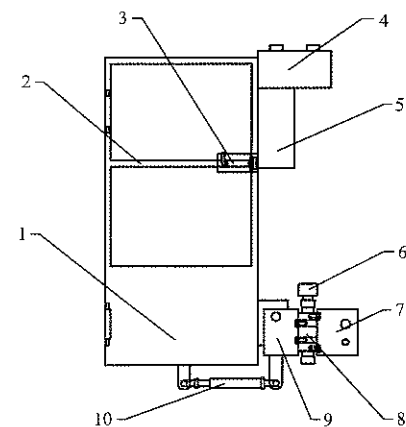
$$h = l_1 \sin \theta_1 + l_2 \sin \theta_2 \quad (3)$$

$$R = l_2 \cos \theta_2 + l_3 + l_4 + l_5 - l_1 \cos \theta_1 \quad (4)$$

Considering the mounting space and based on the design values of operating height (1.2 m) and radius (1.4 m), l_1 was set to 590 mm, l_2 was set to 900 mm, l_3 was set to 80 mm, and l_4 was set to 320 mm. Subsequently, the mounting distances and cylinder displacement of lower-arm cylinder and upper-arm cylinder were set to 380 mm and 160 mm, 510 mm and 230 mm, respectively and at the same time, the maximum θ_1 and θ_2 were 47° and 62°, respectively.

3.2 Manned worktable and leveling device design

As is shown in Figure 5, one side of the guardrails of the manned worktable could be opened for operator to get in conveniently through a bolt. The worktable had enough space for some portable tools and was connected to the upper-arm through the leveling device. The operating box with buttons for lifting, rotating, and leveling was fixed on the front of the worktable.



1. Manned worktable 2. Guardrail 3. Bolt 4. Operating box 5. Control box 6. Leveling hydraulic motor 7. Connection plate of left and right leveling 8. Leveling turbo-worm 9. Connection plate of front and back leveling 10. Leveling cylinder

Figure 5 Structural schematic of the manned worktable

The leveling turbo-worm was driven by the leveling hydraulic motor which could theoretically rotate the manned worktable by 360°, and satisfied the design parameters for left and right leveling operations ($\pm 25^\circ$). On the other hand, when the leveling cylinder telescoped, the manned worktable could rotate around the hinge point between itself and the leveling device to realize front and

back leveling operations. The relationship between leveling angle and displacement of the leveling cylinder is shown in Figure 6 when the manned worktable is leveled to the front, where α_0 is the leveling angle, ($^\circ$); $A(A_0)$ is the hinge point between manned worktable and leveling device; $B(B_0)$ is the hinge point of leveling cylinder; $C_0(C)$ is the hinge points of leveling cylinder; $D_0(D)$ is the points of intersection of $A(A_0)$ and $C_0(C)$ in the horizontal and vertical direction, respectively; a is the horizontal distance, mm; b is the vertical distance, mm; c is the horizontal distance of $A(A_0)$ and $B(B_0)$; l_0 is the mounting distance of leveling cylinder, mm; and Δl is the displacement of leveling cylinder, mm.

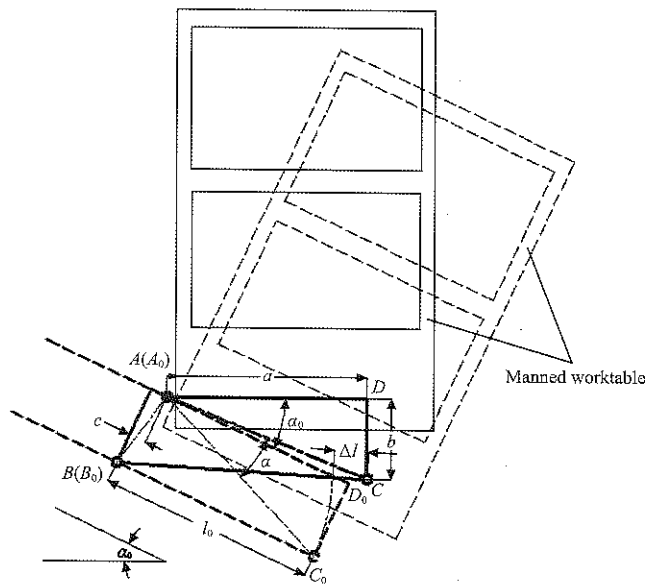


Figure 6 Schematic diagram of relationship between leveling angle and displacement of leveling cylinder

The relationship can be expressed by the following equation as per geometric positions:

$$\Delta l = \sqrt{X^2 + Y^2 - 2XY \cos(\arccos \frac{X^2 + Y^2 - l_0^2}{2XY} + \alpha_0)} - l_0 \quad (5)$$

where, $X^2 = a^2 + b^2$, and $Y^2 = b^2 + c^2$.

Considering the design requirements of the leveling range, the values of a , b , c , and l_0 were set to 430 mm, 180 mm, 35 mm, and 465 mm, respectively. When α_0 was 25° , substituting the values in Equation (5) and solving it, gave $\Delta l = 71$ mm. Meanwhile, it was known that the displacement of the leveling cylinder should be greater than $2\Delta l$, and it was chosen to be 150 mm.

3.3 Operating range

Taking into account the operating characteristics of

the 3-DOF lifting platform, the operating range could be divided into two parts, one was the vertical operating range because of the lifting operation, and another was the horizontal operating range because of the rotating operation. The schematic diagram of the lifting track in the vertical direction shows the operating range of the manned worktable through lifting, and boundaries of the track can be obtained by the graphical method (Wang et al., 2011; Feng et al., 2010), as is shown in Figure 7, where O is the supporting point of the lifting device; OA_j is the base; A_jB_j is the lower-arm; B_jC_j is the middle-arm; D_jE_j is the upper-arm; E_jF_j is the leveling device; F_jG_j is the mounting distance of worktable and leveling device in the vertical direction, m; G_jH_j and $G_j'H_j'$ are the worktable bottom, and $j=1, 2, 3$.

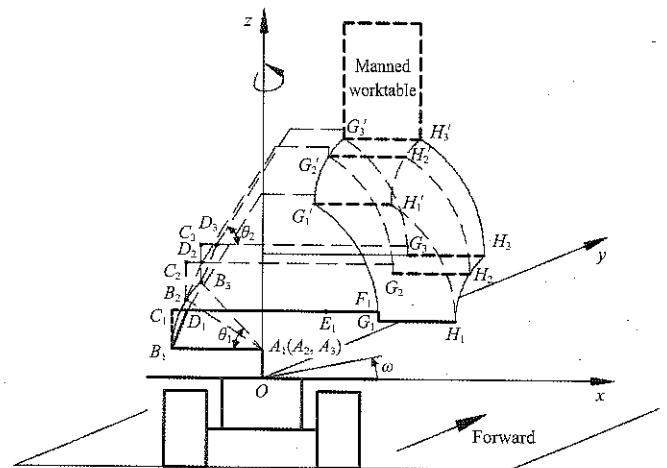


Figure 7 Schematic diagram of lifting track in the vertical direction

When the lifting device was in operation, the manned worktable had three special positions which formed three tracks based on the substitute points of the worktable bottom. When the upper-arm (D_1E_1) was lifted by θ_2 , $G_1H_1H_1'G_1'$ was the operating track of the worktable; when lower-arm (A_2B_2) was lifted by $5\theta_1/8$ and upper-arm (D_2E_2) by θ_2 , $G_2H_2H_2'G_2'$ was the operating track; when lower-arm (A_3B_3) and upper-arm (D_3E_3) were lifted by θ_1 and θ_2 , respectively, $G_3H_3H_3'G_3'$ was the operating track. Obviously, track $G_1H_1, G_1G_1', G_1'G_3', G_3'H_3', H_3'H_3$, and H_3H_1 were the boundaries of the operating ranges in the vertical plane. The maximum operating height were at points G_3' and H_3' , and the maximum and minimum operating radius were at points H_3 and G_1' . When the lifting device was rotating by ω at

any operating height, the track could form a torus, which was the operating range of the worktable in the horizontal plane.

Setting the point A_j as the origin, the right direction of the lifting platform as the x axis, the forward direction as the y axis, and the upward direction from the ground as the z axis, the coordinate system A_jxyz was built. Then, the track G_1H_1 , G_1G_1' , $G_1'G_3'$, $G_3'H_3'$, $H_3'H_3$, and H_3H_1 in the space coordinate system could be expressed by the following equations:

Track G_1H_1 ($\theta_1 = 0^\circ$, $\theta_2 = 0^\circ$, $0^\circ \leq \omega \leq 360^\circ$):

$$\begin{cases} \sqrt{x^2 + y^2} = l_2 + l_3 - l_1 + l_4 + l_{GH} \\ x = (l_2 + l_3 - l_1 + l_4 + l_{GH}) \cos \omega \\ y = (l_2 + l_3 - l_1 + l_4 + l_{GH}) \sin \omega \\ z = l_{BC} - l_{FG} \end{cases} \quad (6)$$

Track G_1G_1' ($\theta_1 = 0^\circ$, $0^\circ \leq \theta_2 \leq 62^\circ$, $0^\circ \leq \omega \leq 360^\circ$):

$$\begin{cases} (\sqrt{x^2 + y^2} + l_1 - l_3 - l_4)^2 + (z - l_{BC} + l_{FG})^2 = l_2^2 \\ \sqrt{x^2 + y^2} = l_3 + l_4 - l_1 + l_2 \cos \theta_2 \\ x = (l_3 + l_4 - l_1 + l_2 \cos \theta_2) \cos \omega \\ y = (l_3 + l_4 - l_1 + l_2 \cos \theta_2) \sin \omega \\ z = l_{BC} - l_{FG} + l_2 \sin \theta_2 \end{cases} \quad (7)$$

where, l_1 is 0.59 m; l_2 is 0.9 m; l_3 is 0.08 m; l_4 is 0.32 m; l_5 is 0.5 m; l_{GH} is from 0 m to 0.5 m; l_{BC} is 0.25 m; and l_{FG} is 0.02 m. Substituting the values and solving the Equations (6) and (7):

Track G_1H_1 ($\theta_1 = 0^\circ$, $\theta_2 = 0^\circ$, $0^\circ \leq \omega \leq 360^\circ$):

$$\begin{cases} \sqrt{x^2 + y^2} = 0.71 + l_{GH} \\ x = (0.71 + l_{GH}) \cos \omega \\ y = (0.71 + l_{GH}) \sin \omega \\ z = 0.23 \end{cases}, \quad 0 \leq l_{GH} \leq 0.5m \quad (8)$$

Track G_1G_1' ($\theta_1 = 0^\circ$, $0^\circ \leq \theta_2 \leq 62^\circ$, $0^\circ \leq \omega \leq 360^\circ$):

$$\begin{cases} (\sqrt{x^2 + y^2} + 0.19)^2 + (z - 0.23)^2 = 0.81 \\ \sqrt{x^2 + y^2} = -0.19 + 0.9 \cos \theta_2 \\ x = (-0.19 + 0.9 \cos \theta_2) \cos \omega \\ y = (-0.19 + 0.9 \cos \theta_2) \sin \omega \\ z = 0.23 + 0.9 \sin \theta_2 \end{cases} \quad (9)$$

Similarly, track $G_1'G_3'$, $G_3'H_3'$, $H_3'H_3$, H_3H_1 could be expressed as:

Track $G_1'G_3'$ ($0^\circ \leq \theta_1 \leq 47^\circ$, $\theta_2 = 62^\circ$, $0^\circ \leq \omega \leq 360^\circ$):

$$\begin{cases} (\sqrt{x^2 + y^2} - 0.82)^2 + (z - 1.02)^2 = 0.35 \\ \sqrt{x^2 + y^2} = 0.82 - 0.59 \cos \theta_1 \\ x = (0.82 - 0.59 \cos \theta_1) \cos \omega \\ y = (0.82 - 0.59 \cos \theta_1) \sin \omega \\ z = 1.02 + 0.59 \sin \theta_1 \end{cases} \quad (10)$$

Track $G_3'H_3'$ ($\theta_1 = 47^\circ$, $\theta_2 = 62^\circ$, $0^\circ \leq \omega \leq 360^\circ$):

$$\begin{cases} \sqrt{x^2 + y^2} = 0.42 + l_{GH} \\ x = (0.42 + l_{GH}) \cos \omega \\ y = (0.42 + l_{GH}) \sin \omega \\ z = 1.43 \end{cases}, \quad 0 \leq l_{GH} \leq 0.5m \quad (11)$$

Track $H_3'H_3$ ($\theta_1 = 47^\circ$, $0^\circ \leq \theta_2 \leq 62^\circ$, $0^\circ \leq \omega \leq 360^\circ$):

$$\begin{cases} (\sqrt{x^2 + y^2} - 0.5)^2 + (z - 0.66)^2 = 0.81 \\ \sqrt{x^2 + y^2} = 0.5 + 0.9 \cos \theta_2 \\ x = (0.5 + 0.9 \cos \theta_2) \cos \omega \\ y = (0.5 + 0.9 \cos \theta_2) \sin \omega \\ z = 0.66 + 0.9 \sin \theta_2 \end{cases} \quad (12)$$

Track H_3H_1 ($0^\circ \leq \theta_1 \leq 47^\circ$, $\theta_2 = 0^\circ$, $0^\circ \leq \omega \leq 360^\circ$):

$$\begin{cases} (\sqrt{x^2 + y^2} - 1.8)^2 + (z - 0.23)^2 = 0.35 \\ \sqrt{x^2 + y^2} = 1.8 - 0.59 \cos \theta_1 \\ x = (1.8 - 0.59 \cos \theta_1) \cos \omega \\ y = (1.8 - 0.59 \cos \theta_1) \sin \omega \\ z = 0.23 + 0.59 \sin \theta_1 \end{cases} \quad (13)$$

The lifting operation range around the fruit trees on both sides of the vertical plane is shown in Figure 8a, and its value is set as S . The operating range for the rotating operation at maximum radius is set as S' , as is shown in Figure 8b.

S and S' can be calculated from the Equations (14) and (15):

$$\begin{aligned} S &= S_{G_1G_1'H_1} + S_{G_1'G_3'H_3'} + S_{H_3'H_3} \\ &= l_5 l_2' \sin \theta_{2\max} + l_5 l_1' \sin \theta_{1\max} + \end{aligned} \quad (14)$$

$$4l_1' l_2' \sin \frac{\theta_{1\max}}{2} \sin \frac{\theta_{2\max}}{2} \sin \frac{\theta_{1\max} + \theta_{2\max}}{2}$$

$$S' = \pi [R_{\max}^2 - (R_{\max} - l_5)^2] \quad (15)$$

where, l_1' is equal to the length of lower-arm, m; l_2' is equal to the length of upper-arm, m; $\theta_{1\max}$ is the maximum lifting angle of lower-arm, ($^\circ$); $\theta_{2\max}$ is the maximum lifting angle of upper-arm, ($^\circ$); and R_{\max} is the maximum operating radius, m.

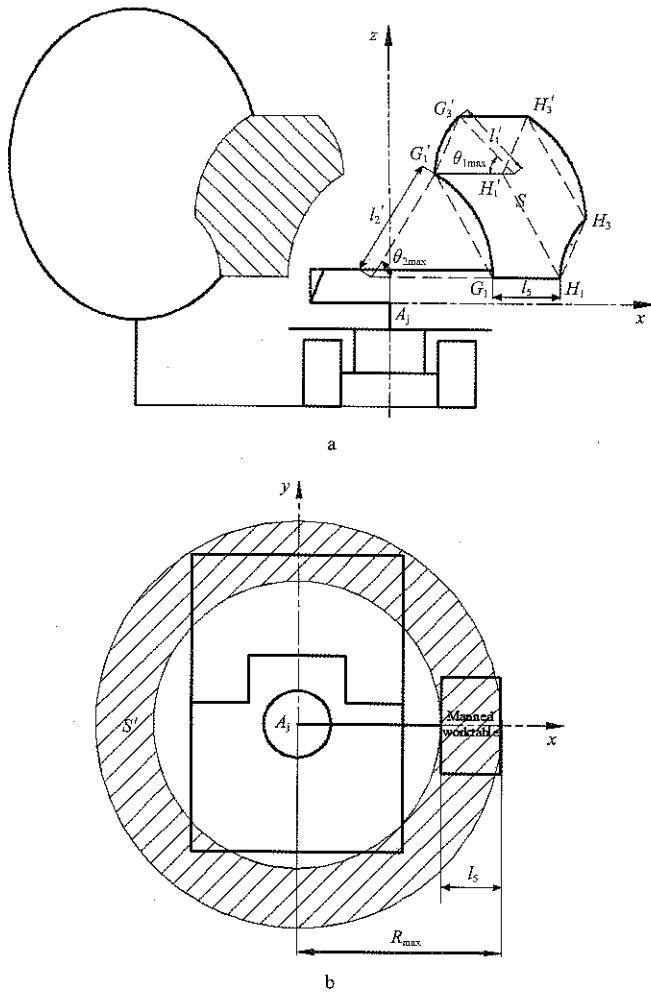


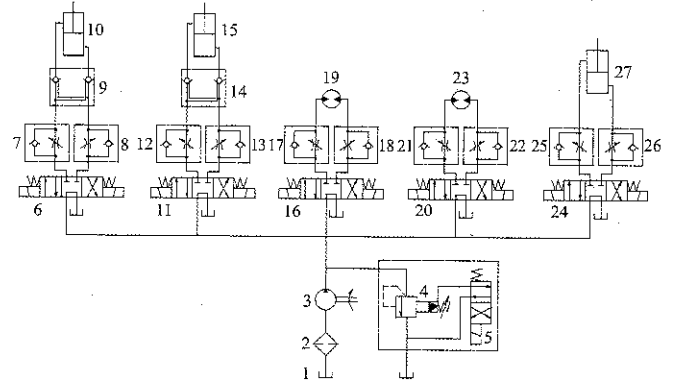
Figure 8 Schematic diagram of operating range of the manned worktable

Substituting the values in Equations (14) and (15) and solving them yields an operating range for lifting and rotating of about 1.9 m² and 3.6 m². Compared to other machines, this lifting platform, thus, has a larger operating range.

3.4 Hydraulic system design

The hydraulic system was powered by the engine which was connected to the gear pump through the belt transmission. A clutch was fixed to the gear pump to switch the power transmission on and off. As is shown in Figure 9, the gear pump supplied oil to every hydraulic element. A two position four-way solenoid directional valve was always open and set to control the gear pump unloading. As the hydraulic system only comprised three kinds of action - lifting, rotating, and leveling and no other special actions, double action hydraulic cylinder and double action quantitative hydraulic motor were selected. The work flow was adjusted by one-way throttle valve. When lifting platform was operational in the

orchards, the system needed to start and stop frequently to change the operating position of the manned worktable; however, in order to keep the stability of the operation, hydraulic locks were adopted on the branches of the lifting cylinders to realize static locking.



1. Tank 2. Filter 3. Gear pump 4. Piloted relief valve 5. Two position four-way solenoid directional valve 6, 11, 16, 20, 24. Three position four-way solenoid directional valve 7, 8, 12, 13, 17, 18, 21, 22, 25, 26. Throttle valve 9,14. Hydraulic lock 10,15. Lifting cylinder 19. Rotating hydraulic motor 23. Leveling hydraulic motor 27. Leveling cylinder

Figure 9 Schematic diagram of the hydraulic system

Considering the type of equipment (Wang et al., 2016), the maximum working pressure was set to 16 MPa. The outer diameter and inner diameter of the leveling cylinder were selected as 50 mm and 35 mm as per the requirements of 1.25 times the maximum load. The rotating speed of lifting device and leveling turbo-worm needed to be slower for the operator to work comfortably; hence, they were set from 0.5 r/min to 1 r/min. In addition, the working parameters of other elements and different component selections are shown in Table 2.

Table 2 Model of hydraulic and drive components

Project	Model
Lower-arm cylinder	50×35×160
Upper-arm cylinder	50×35×230
Leveling cylinder	50×35×150
Leveling turbo-worm	SE3
Slewing bearing	SE12
Rotating hydraulic motor	BMI-160-H
Leveling hydraulic motor	HMM-50
Gear pump	CBT-E304
Hydraulic lock	YS6-03A
Solenoid relief valve	DBW-10B-2B2
Solenoid directional valve	DSG-02-3C2

4 Materials and methods

4.1 Experimental conditions

In accordance with the design parameters of a 3-DOF

lifting platform, the prototype was developed as is shown in Figure 10. It has been known that the rated speed of the engine is 2200 r/min, and the lifting platform is able to work in the middle throttle. Experiments including operating parameters experiment, operating effect on fruit trees experiment, leveling and tilting stability experiment were carried out to analyze the performance of the 3-DOF lifting platform for hilly orchards. The experiments were conducted in October and November 2016 on the field of College of Engineering, Nanjing Agricultural University.

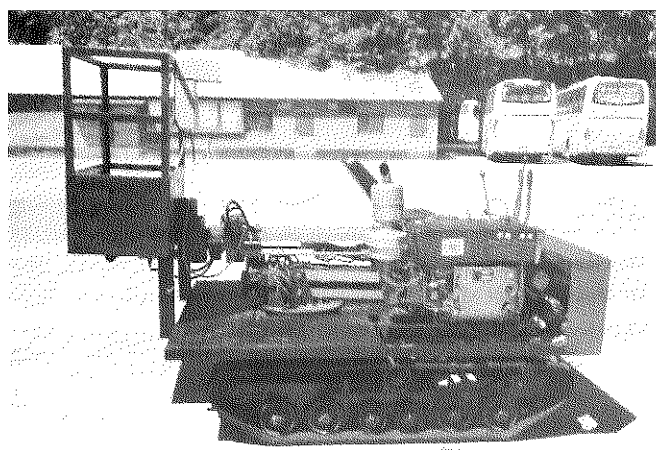


Figure 10 Prototype of 3-DOF lifting platform for hilly orchards

4.2 Experimental methods

4.2.1 Operating parameters experiment

Operating parameters experiment used parameters such as the speed of lifting operation, rotating operation, and leveling operation, and test of maximum operating height and radius. This can be referenced from the "Scissors elevating platforms - Testing method" (JB/T 9229.3-1999).

4.2.2 Operating effect on fruit trees experiment

Three fruit trees with different growth parameters (tree height, trunk height, and tree crown) were selected, and marked 1, 2, and 3. The canopies were divided into three vertical layers, which were marked as a , b , and c , and every layer was divided into a_k , b_k , and c_k ($k=1, 2, 3, 4, 5$). A total of 16 markers within the top point (T) of the tree were set as experimental positions (Figure 11), and label papers were pasted on the leaves at the corresponding positions. The position of the parked lifting platform was 2 m or 2.5 m away from the fruit tree.

The experimental points were marked with Y (Yes) or

N (No) depending on whether the operator could reach them or not without any tools when lifting and rotating as is shown in Figure 12.

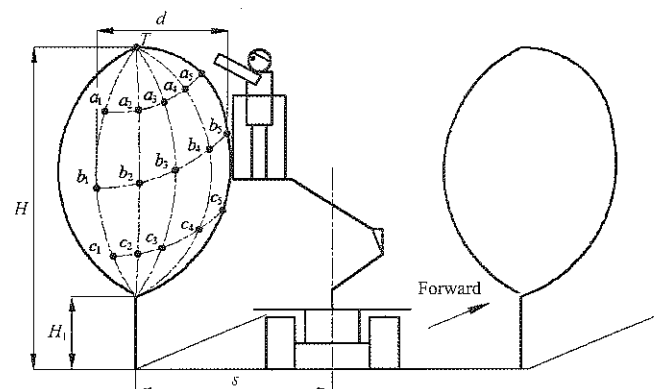


Figure 11 Schematic diagram of experiment of the operating range



Figure 12 Field experiment in progress

4.2.3 Leveling experiment

When the 3-DOF lifting platform was parked on the slope, different operating positions of the manned worktable resulted in different tilt angles and directions. As a result, there were different leveling actions including front, back, left and right. A tilting table was used to simulate different angles of slopes where the lifting platform was parked on and was fixed by safety rope. The operating height was 0.8 m and the tilt angles of the tilting table were 6° and 18° . The lifting device was rotated counterclockwise to 0° , 0° - 90° , 90° , 90° - 180° , 180° , 180° - 270° , 270° , 270° - 360° . Thus, the manned worktable was leveled using the bubble level in X and Y

direction. The error in the leveling operation could be measured by a digital inclinometer. In addition, the right hand side of the manned worktable was set as the positive direction of the X axis and the front as the positive direction of the Y axis.

4.2.4 Tilting stability experiment

The tilting stability was one of the most important features of the 3-DOF lifting platform, because different parking positions with different operating heights, different operating radii and different loads resulted in different tilting angles, and could make working on the lifting platform safe or unsafe on a slope. The tilting stability performance was characterized by the maximum tilting angle that could be measured. Using the “Tri-wheel vehicles and low-speed goods vehicles-Test method of maximum stable side-inclination” (GB/T 19133-2015), the operating environment was simulated with the following parameters: 8 parking positions with 0°, 45°, 90°, 135°, 180°, 225°, 270°, and 315° between the forward direction and the slope direction; 4 operating heights of 0 m, 0.4 m, 0.8 m, and 1.2 m; and 4 loadings of 0 kg, 50 kg, 100 kg, and 150 kg. Due to the manned worktable along the slope being always the most easily tilting position no matter where the lifting platform was parked, the experiment positions were set as is shown in Figure 13. The maximum angle of tilting test table is 30°, the length of table is 4 m, the width is 5 m, and the start-stop mode is the electric control.

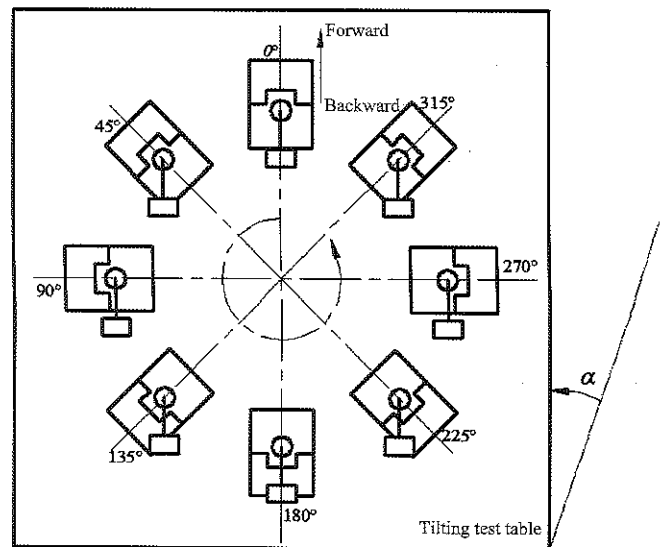


Figure 13 Schematic diagram of experimental positions

5 Results and discussion

5.1 Operating parameters

The experimental results are shown in Tables 3 and 4. Lifting, rotating and leveling had lower operating speeds which satisfied the design requirements, and the lifting speed was less than 0.4 m/s. Meanwhile, operating with full load always led to slower speeds. The maximum operating height was 1.2 m, and the height from the ground was 2.1 m at the same time. When the operating height was above 0.62 m, the lifting device could rotate 360° with a maximum radius of 1.42 m, for which the operating range was about 3.6 m². However, at operating height of less than 0.62 m, it could only rotate 180° because of space limitations.

Table 3 Speed of lifting, rotating and leveling

Load, kg	Lifting, m·s ⁻¹		Falling, m·s ⁻¹		Rotating, r·min ⁻¹		Leveling, rad·s ⁻¹			
	Upper-arm	Lower-arm	Upper-arm	Lower-arm	Left	Right	Front	Back	Left	Right
0	0.065	0.063	0.085	0.056	0.58	0.58	0.071	0.065	0.074	0.067
150	0.056	0.056	0.068	0.067	0.57	0.56	0.055	0.052	0.069	0.065

Table 4 Parameters of operating height and radius

Project	Maximum operating height/m	Maximum height from the ground/m	Rotating in 360°	
			Maximum operating radius, m	Operating height, m
Parameters	1.2	2.1	1.42	0.62

5.2 Operating effect on fruit trees

Growth parameters of fruit trees selected are shown in Table 5. Due to the shape of the fruit trees being approximately ellipsoidal, the layer *b* had a larger crown than layer *a* and *c*. The markers *b*₁, *b*₅, *c*₁ and *c*₅ were the

most difficult positions for the operator to reach. In addition, the lifting platform could only move in a small range to adjust the boundaries of the crown. The layer *c* had a lower distance from the ground, so other operator could stand on the ground to finish the operations for

markers c_1 and c_5 . When the distance from the lifting platform to the fruit trees was 2 m, the operating effect was better than when the distance was 2.5 m. Overall, the

operating range could almost cover entire canopies. Thus, the 3-DOF lifting platform had a good operating effect on fruit trees when the distance between them was 2 m.

Table 5 Operating effect on fruit trees

No.	Growth parameters			Distance, m	Operating effect															
	Tree height, m	Trunk height, m	Tree crown, m		T	a_1	a_2	a_3	a_4	a_5	b_1	b_2	b_3	b_4	b_5	c_1	c_2	c_3	c_4	c_5
1	3.24	0.62	2.3	2	Y	Y	Y	Y	Y	Y	Y	Y	Y	Y	N	N	Y	Y	Y	N
				2.5	Y	N	Y	Y	Y	N	N	Y	Y	Y	N	N	Y	Y	Y	N
2	3.35	0.65	2.8	2	Y	Y	Y	Y	Y	N	Y	Y	Y	N	N	Y	Y	Y	N	
				2.5	N	N	Y	Y	Y	N	N	Y	Y	Y	N	N	Y	Y	Y	N
3	3.46	0.72	2.7	2	Y	Y	Y	Y	Y	Y	Y	Y	Y	N	Y	Y	Y	Y	Y	
				2.5	Y	N	Y	Y	Y	N	N	Y	Y	Y	N	N	Y	Y	Y	N

5.3 Leveling error

It can be seen from Table 6 that different rotating positions of the manned worktable had different leveling actions. Irrespective of the angle of slope being 6° or 18°, the leveling errors for the leveling actions were all less than 0.4°, which is negligible. Thus, using a leveling cylinder and leveling turbo-worm to keep the manned worktable horizontal according to the bubble level can be considered to have a relatively high accuracy.

5.4 Maximum tilting angle

The experimental results in Table 7 indicate that the maximum tilting angle decreased with an increase in load, for the same parked position and operating height. Moreover, the maximum tilting angle decreased and then increased with an increase in operating height. The angles of different parked positions, for different operating heights and different loads were from 19.3° to 30°, but some of the experimental angles were above 30° which were out of the measured range of the tilting table. Thus, the experiment results satisfied the design requirements,

and the proposed 3-DOF lifting platform has a better tilting stability and can adapt to slope conditions of 5° to 20° in hilly orchards.

Table 6 Leveling error

Angle of slope, (°)	Rotating positions, (°)	Leveling actions	Dip angles, (°)		Leveling error, (°)	
			X axis	Y axis	X axis	Y axis
6	0	Front	0	-6	-	0.2
	0-90	Right, Front	-3.2	-5.7	0.2	0.1
	90	Right, Front	-7.3	-1.4	0.4	0.1
	90-180	Right, Back	-1.9	4.6	0.1	0.2
	180	Back	0	6	-	0.3
	180-270	Left, Back	4.1	4.3	0.4	0.3
	270	Left, Front	7.6	-1.3	0.3	0.2
	270-360	Left, Front	1.6	-2.1	0.2	0.2
18	0	Front	0	-18	-	0.3
	0-90	Right, Front	-13.5	-14.2	0.2	0.3
	90	Right, Front	-18.6	-2.7	0.3	0.1
	90-180	Right, Back	-11.5	12.3	0.2	0.2
	180	Back	0	18	-	0.2
	180-270	Left, Back	10.7	14.8	0.1	0.3
	270	Left, Front	18.8	-1.3	0.3	0.1
	270-360	Left, Front	12.5	-14.1	0.2	0.4

Table 7 Maximum tilting angle experimental value

Parking Position, (°)	Maximum tilting angle of different loads at various operating heights, (°)															
	0 kg				50 kg				100 kg				150 kg			
	0 m	0.4 m	0.8 m	1.2 m	0 m	0.4 m	0.8 m	1.2 m	0 m	0.4 m	0.8 m	1.2 m	0 m	0.4 m	0.8 m	1.2 m
0	>30	>30	29.2	>30	>30	27.4	25.7	26.1	27.4	23.9	22.6	23.7	26.1	20.4	19.3	21.4
45	>30	>30	>30	>30	>30	>30	27.8	28.1	>30	26.3	24.1	25.2	26.7	23.1	22.8	23.3
90	>30	>30	>30	>30	29.5	29.1	28.2	28.5	28.8	27.4	24.9	25.6	27.8	25.3	23.8	24.5
135	*	>30	>30	>30	*	>30	>30	>30	*	>30	>30	>30	*	28.8	27.2	28.1
180	*	*	>30	>30	*	*	>30	>30	*	*	>30	>30	*	*	28.4	29.8
225	*	>30	>30	>30	*	27.8	26.3	26.8	*	26.5	25.3	25.7	*	25.2	23.9	24.6
270	*	>30	29.4	>30	*	27.1	25.7	26.2	*	24.9	24.1	24.3	*	22.5	20.7	21.9
315	>30	>30	>30	>30	>30	>30	29.2	>30	>30	>30	25.4	26.1	27.6	24.5	21.2	22.1

Note: * means the position where the manned worktable can not reach.

6 Conclusions

A 3-DOF lifting platform was developed to improve the level of mechanization of processes such as picking, pruning, and bagging in hilly orchards and to solve the problem of lack of equipment for such processes. The lifting device which was one of the most important parts, was developed using a folding-arm mechanism. In addition, a leveling device was designed to keep the manned worktable horizontal on different terrains. The structural parameters and operating parameters were determined based on design requirements and the geometric parameters of fruit trees that were collected by visiting orchards on hilly lands. Subsequently, experiments were carried out to evaluate the performance of the proposed lifting platform.

The experimental results indicated that the operations of lifting, rotating and leveling were slow and smooth, the maximum operating height was 1.2 m, the lifting device could rotate 360° at a maximum operating radius of 1.42 m when operating height was above 0.62 m, and as a result, the operating range was about 3.6 m² at the same time. It was also confirmed that operator standing on the manned worktable could reach almost any position on the fruit trees. Compared to other current mechanical devices, the proposed 3-DOF lifting platform has the advantages of having a larger operating range, more operational flexibility and being more efficient when parked.

Furthermore, the error in any leveling action was less than 0.4°, which is negligible and the leveling device can thus be considered to have a relatively high accuracy. The maximum tilting angle at different parked positions, different operating heights and different loads was from 19.3° to 30°, which was as per the design requirements and could be adapted to slope conditions with an angle ranging from 5° to 20° in hilly orchards. The proposed 3-DOF lifting platform for hilly orchards, thus, had a better tilting stability performance compared to current machinery.

Acknowledgements

This study was supported by Co-Innovation Center of the Intelligent Management and Equipment for Orchard on the Hilly Land in South China (JX2014XCHJ02).

[References]

- [1] Cao, F. Y., Z. L. Zhou, and H. S. Jia. 2007. Research summarization on simulation of turning performance of tracked vehicle. *Transactions of the Chinese Society for Agricultural Machinery*, 38(1): 185–188. (In Chinese with English abstract)
- [2] Chang, Y. H., X. L. Lv, , Lv Xiaolan, J. Lin, X. Y. Xue, and Z. H. Wang. 2013. Present state and thinking about development of orchard mechanization in China. *Journal of Chinese Agricultural Mechanization*, 34(6): 21–25. (In Chinese with English abstract)
- [3] Ding, S. M., X. M. Fu, X. Y. Xue, L. F. Zhou, and X. L. Lv. 2013. Design of power chassis for low self-propelled orchard sprayer. *Transactions of the Chinese Society for Agricultural Machinery*, 44(Supp.1): 101–106. (In Chinese with English abstract)
- [4] Feng, Q. C., C. Ji, J. X. Zhang, and W. Li. 2010. Optimization design and kinematic analysis of cucumber-harvesting-robot manipulator. *Transactions of the Chinese Society for Agricultural Machinery*, 41(Supp.1): 244–248. (In Chinese with English abstract)
- [5] GB/T 19133-2015 Tri-wheel vehicles and low-speed goods vehicles-Test method of maximum stable side-inclination. National Standards of the People's Republic of China.
- [6] Hong, T. S., Z. Yang, S. R. Song, Y. Q. Zhu, X. J. Yue, and J. Su. 2010. Mechanization of citrus production. *Transactions of the Chinese Society for Agricultural Machinery*, 41(12): 105–110. (In Chinese with English abstract)
- [7] JB/T 9229.3-1999 Scissors elevating platforms-Testing method. Machinery Industry Standards of the People's Republic of China
- [8] Liu, D. W. 2013. Design and experimental research on lifting platform in citrus orchard. Changsha: Hunan Agricultural University.
- [9] Liu, X. N., H. T. Zhu, and H. T. Ba. 2009. Development of a Faun LG1 type multifunctional orchard operating machine. *Xinjiang Agricultural Mechanization*, 2(1): 42–44. (In Chinese with English abstract)
- [10] Liu, D. W., F. P. Xie, X. Li, X. L. Wang, and T. Mei. 2014. Citrus canopy shape and picking platform mechanical adaptability relationship with the inexact research. *Acta Agriculturae Universitatis Jiangxiensis*, 36(5): 1091–1095. (In Chinese with English abstract)
- [11] Li, Q., Y. P. Song, D. S. Gao, X. C. Li, and H. R. Su. 2012. Status and development of orchard machinery in China. *Agricultural Equipment & Vehicle Engineering*, 247(2): 1–3.
- [12] Liu, D. W., F. P. Xie, X. Li, and X. L. Wang. 2015. Design and experiment of small lifting platform in orchard. *Transactions of the CSAE*, 31(3): 113–121. (In Chinese with English abstract)

- [13] Miao, M., H. Yuan, X. G. Song, Z. C. Shen, and W. Zhao. 2013. Folding-boom aerial working vehicle tracking and control. *Chinese Journal of Construction Machinery*, 11(4): 320–323. (In Chinese with English abstract)
- [14] Qiu, W., W. M. Ding, X. C. Wang, Y. Gong, and X. X. Zhang. 2012. 3WZ-700 self-propelled air-blowing orchard sprayer. *Transactions of the Chinese Society for Agricultural Machinery*, 43(4): 26–30. (In Chinese with English abstract)
- [15] Qiu, W., C. D. Sun, X. L. Lv, Y. L. Chen, and W. M. Ding. 2016. Effects of spraying mode and application rate on pesticide deposition on fruit trees. *International Agricultural Engineering Journal*, 25(3): 182–196.
- [16] Sun Z. J. 2012. Design and research of crawler multifunctional orchard operating Platform. Baoding: Hebei Agricultural University.
- [17] Tang J. W., W. P. Liu, D. G. Liu, and G. Cheng. 2006. An analysis of steering track for tracked vehicle at inaccurate steering. *Acta Armamentarii*, 27(5): 779–783.
- [18] Wang X. L., F. P. Xie, D. W. Liu, X. Li, and W. Lu. 2014. Citrus canopy shape and picking platform mechanical adaptability relationship with the inexact research. *Journal of Hunan Agricultural University Natural Sciences*, (5): 548–551. (In Chinese with English abstract)
- [19] Wang, Z. 2011. Small multi-function remote control power platform. *Agricultural Equipment & Technology*, (3): 39.
- [20] Wang, Y., Q. H. Yang, G. J. Bao, Y. Yi, and L. B. Zhang. 2011. Optimization design and experiment of fruit and vegetable picking manipulator. *Transactions of the Chinese Society for Agricultural Machinery*, 42(7): 192–195. (In Chinese with English abstract)
- [21] Wang, P. F. 2013. The control system design and research of orchard operating platform. Baoding: Hebei Agricultural University.
- [22] Wang, H. B., F. Z. Liu, D. X. Wang, H. Zhai, and Y. P. Du. 2013. Review on research, development and application of orchard machinery in China. *Journal of Fruit Science*, 30(1): 165–170.
- [23] Wang, J. C. 2013. Design on hanging operating platform for hilly orchards. Tai'an: Shandong Agricultural University.
- [24] Wang, B. S., W. Z. Wang, M. M. Wang, D. F. Zhong, and J. Chen. 2016. Design and experiment of full hydraulic drive high clearance tracked vehicle. *Transactions of the Chinese Society for Agricultural Machinery*, 47(Supp.1): 471–476. (In Chinese with English abstract)
- [25] Zhang, X. H., Z. Y. Jiang, G. Q. F, and L. L. Cao. 2014. Self-propelled crawler directional air-blowing orchard sprayer. *Transactions of the Chinese Society for Agricultural Machinery*, 45(8): 117–122. (In Chinese with English abstract)
- [26] Zhao, J. Z., F. C. Wang, B. Yu, and D. C. Wang. 2014. Research on all-terrain profiling crawler power chassis. *Transactions of the Chinese Society for Agricultural Machinery*, 45(9): 20–24. (In Chinese with English abstract)
- [27] Zhou, L. F., X. M. Fu, W. M. Ding, S. M. Ding, J. Chen, and Z. J. Chen. 2015. Design and experiment of combined disc air-assisted orchard sprayer. *Transactions of the CSAE*, 31(10): 64–71. (In Chinese with English abstract)